Chromium(II) Amides: Synthesis and Structures†

Jilles J. H. Edema,[a] Sandro Gambarotta,*[,b] Auke Meetsma,[a] Anthony L. Spek,[c] Wilberth J. J. Smeets[c] and Michael Y. Chiang[d]

[a] *Laboratorium voor Anorganische Chemie, Rijksuniversiteit Groningen, Nijenborgh 16, 9747 AG Groningen, The Netherlands*

[b] *Department of Chemistry, University of Ottawa, Ottawa, Ontario K1N 6N5, Canada*

[c] *Vakgroep Algemene Chemie, Afdeling Kristal-en Structuurchemie, Rijksuniversiteit Utrecht, Padualaan 8, 3584 CH Utrecht, The Netherlands*

[d] *Chemistry Department, Washington University, One Brooking Drive, St. Louis, MO, 63130, USA*

A novel class of mono- and di-meric chromium(II) amides has been prepared and characterized. Reaction of $[CrCl_2(thf)_2]$ (thf = tetrahydrofuran) with 2 equivalents of $M(NR_2)$ (R = C_6H_{11}, Pr^i, Ph, or phenothiazinyl; M = Li or Na) allowed the formation of the homoleptic amides $[\{Cr(\mu\text{-}NR_2)(NR_2)\}_2]$ (R = Ph **1a**, C_6H_{11} **1b** or Pr^i **1c**). The reaction is followed by co-ordination of a Lewis base which, although preserving the $Cr_2(NR_2)_2$ core, remarkably elongated the Cr···Cr distance forming $[\{Cr(\mu\text{-}NR_2)(NR_2)L\}_2]$ (R = Ph, L = thf **2**). Facile cleavage to give the square-planar monomeric species $[Cr(NR_2)L_2]$ (R = Ph, L = pyridine **3a**, thf **3b**; NR_2 = phenothiazinyl, L = thf **3c**) occurred upon treatment with an excess of co-ordinating solvent. Reaction with an excess of $M(NR_2)$ led to the formation of anionic chromium(II) square-planar metalates $[M_2Cr(NR_2)_4L_2]$ (R = Ph, M = Na, L = thf **4a**; R = Et, M = Li, L = thf **4b** or pyridine **4c**). A dimeric species with a very short Cr···Cr contact $[\{Cr[N(C_5H_4N\text{-}2)_2]_2\}_2]\cdot 2dmf$ (dmf = dimethylformamide) **5b** has been obtained involving a unique three-centre chelating geometry of the bridging amide ligand. The crystal structures of compounds **1b**, **2**, **3a**, **3c**, **4c** and **5b** have been determined.

Anionic organic amides obtained by deprotonation of secondary amines may act as versatile ligands in the preparation and stabilization of early transition metals in low oxidation states. Several features of these ligands, such as electronic flexibility, the possibility of fine tuning of the steric hindrance and of introducing chiral groups, and the ability to bridge two or more transition metals, make their utilization particularly promising. In agreement with these expectations, activation of C–H bonds,[1] preparation of the full series of lanthanides in unusual co-ordination geometries,[2] and isolation of a series of exotic Group 4 metal dinitrogen complexes[3,4] are among the most significant results recently achieved using sterically demanding amides. However, despite the great potential for both synthesis and chemical reactivity studies, not much work has been done on the chemistry of low-valent early transition-metal amides, since the pioneering work of Bradley and Lappert in the 1970s.[5] While the chemistry of low-valent Group 3–5 transition-metal amides remains poorly developed,[6] organic amides have been widely and successfully used in the chemistry of low-valent molybdenum and tungsten achieving some spectacular successes in cluster chemistry[7] and the activation of small molecules.[8]

The chemistry of chromium amides and in particular of the oxidation state +II is, by way of contrast, limited to three diverse examples.[9] This is despite some attractive characteristics of divalent chromium and, in particular, a unique ability to form dinuclear cores with unusually short Cr···Cr contacts, which makes chromium(II) complexes ideal substrates for clusterification reactions. In this respect, since the nature of the donor atom and the geometry of the organic moiety are the properties of bridging ligands which are likely to be the most important in determining the stability of di- and poly-metallic cores, it is important to carry out a systematic synthetic and structural study on the chemistry of divalent chromium with monodentate ligands without special chelating abilities. The ultimate goal is to clarify the intriguing role of bridging donor atoms in determining both the occurrence of short Cr···Cr contacts and the magnetic properties of the metal, and empirically to evaluate the effective contribution of Cr···Cr bonds to the stability of dinuclear frameworks. Therefore, as a continuation and extention of our work in this field,[10] we have now investigated the structural features of a class of monomeric and dimeric chromium(II) amides, with the dual purpose of developing the poorly known chemistry of chromium(II) monodentate amides,[9] and hopefully gaining insight into how the nitrogen of organic amides might affect the geometry of dichromium species.

Experimental

All operations were performed under an inert atmosphere (N_2 or Ar) using standard Schlenk techniques, or in a nitrogen-filled dry-box (Vacuum Atmosphere). The compounds $[CrCl_2(thf)_2]$ (thf = tetrahydrofuran),[11] $[Cr(mes)_2(thf)_3]$ (mes = mesityl)[12] and $[Li_4Cr_2Me_8(thf)_4]$[12d,e] were prepared according to published procedures; $N(C_6H_{11})_2H$, NEt_2H and NPr^i_2H were chromatographed over Al_2O_3 and distilled over molten potassium and 2-methylaminopyridine, di-2-pyridylamine, phenothiazine and NPh_2H were used as received (Aldrich). Infrared spectra were recorded on a Perkin Elmer 283 instrument from Nujol mulls prepared in a dry-box. Elemental analyses were carried out at the Microanalytical Department of the Chemistry Department at the Rijksuniversiteit Groningen. Samples for magnetic susceptibility measurements were weighed inside a dry-box equipped with a microanalytical balance, and sealed into a specially designed Teflon capsule. Data were recorded at variable temperatures in the range 100–298 K by using a Faraday balance (Oxford Instruments) interfaced with an Apple II computer. Plots of $1/\chi_M$ against T/K were in

† *Supplementary data available:* see Instructions for Authors, *J. Chem. Soc., Dalton Trans.*, 1993, Issue 1, pp. xxiii–xxviii.

satisfactory agreement with the Curie–Weiss law in the case of complexes **1**, **2** and **5**. Magnetic moments were calculated following standard methods[13] and corrections for underlying diamagnetism were applied to the data.[14] Magnetic moments of all the other complexes were measured at room temperature by using a Johnson-Mathey magnetic susceptibility balance.

$[\{Cr(\mu\text{-}NPh_2)(NPh_2)\}_2]$ **1a**.—A red greenish solution of $[\{Cr(\mu\text{-}NPh_2)(NPh_2)(thf)\}]$ **2** prepared as below (3.40 g, 3.78 mmol) in toluene (100 cm^3) was refluxed for 2 h. After evaporation to dryness, the residue was redissolved in toluene (100 cm^3), refluxed for 2 h and subsequently evaporated to dryness. After repeating this procedure three times, light green crystals of compound **1a** (1.65 g, 2.13 mmol, 55%) were formed upon concentrating and cooling the resulting toluene solution (Found: C, 74.10; H, 5.20; Cr, 13.35; N, 7.10. Calc. for $C_{24}H_{20}CrN_2$: C, 74.2; H, 5.20; Cr, 13.40; N, 7.20%). IR (Nujol mull, KBr, cm^{-1}): 1610m, 1570s, 1550m, 1330s, 1295s, 1260s, 1210s, 1165w, 1120s, 1000s, 1030w, 1000w, 920w, 895s, 850m, 790w, 740m, 720m, 670d (w), 685s, 670s, 610w and 530m. μ_{eff} = 2.67.

$[\{Cr[\mu\text{-}N(C_6H_{11})_2][N(C_6H_{11})_2]\}_2]$ **1b**.—A solution of LiMe in diethyl ether (4.5 cm^3, 1.74 mol dm^{-3}, 7.8 mmol) was added to a cooled solution of $N(C_6H_{11})_2H$ (1.97 g, 8.1 mmol) in thf (30 cm^3). After 15 min of stirring, solid $[CrCl_2(thf)_2]$ (1.02 g, 3.8 mmol) was added. The resulting dark green suspension was stirred for 3 h and then filtered. Blue-green crystals of compound **1b** separated (1.11 g, 2.7 mmol, 71%) upon addition of ether (20 cm^3) (Found: C, 69.95; H, 10.80; Cr, 12.60; N, 6.85. Calc. for $C_{24}H_{44}CrN_2$: C, 69.85; H, 10.75; Cr, 12.60; N, 6.80%). IR (Nujol mull, KBr, cm^{-1}): 1460s, 1330m, 1230m, 1130m, 1100m, 1070s, 1065s, 1050m, 1030s, 975m, 960s, 905w, 880s, 830s, 790w and 670m. μ_{eff} = 2.62.

$[\{Cr(\mu\text{-}NPr^i_2)(NPr^i_2)\}_2]$ **1c**.—A solution of LiMe (8 cm^3, 1.4 mol dm^{-3}, 11.2 mmol) in ether was added to a cooled solution of NPr^i_2H (1.13 g, 11.1 mmol) in thf (25 cm^3). After 10 min of stirring the addition of solid $[CrCl_2(thf)_2]$ (1.3 g, 5.2 mmol) turned the solution green-brown. After 5 h of stirring the solvent was removed *in vacuo* and the residue was crystallized at −80 °C from pentane (10 cm^3), yielding deep green crystals of compound **1c** (0.96 g, 1.9 mmol, 73%) (Found: C, 57.10; H, 11.20; Cr, 20.45; N, 11.50. Calc. for $C_{12}H_{28}CrN_2$: C, 57.10; H, 11.20; Cr, 20.60; N, 11.10%). IR (Nujol mull, KBr, cm^{-1}): 1375s, 1360s, 1335m, 1310w, 1155s, 1150m, 1100s, 990m, 970w, 920s, 840m, 805m, 635m, 550m, 500w, 480w and 420w. μ_{eff} = 2.30.

$[\{Cr(\mu\text{-}NPh_2)(NPh_2)(thf)\}_2]$ **2**.—A purple solution of $[Cr(NPh_2)_2(thf)_2]$ (0.73 g, 1.27 mmol) in toluene (75 cm^3) was refluxed for 45 min. The resulting green solution was concentrated to a small volume (10 cm^3) by distilling off the toluene at atmospheric pressure. The solution was slowly allowed to cool to room temperature. The colour turned brown, and red crystals of compound **2** (0.323 g, 0.35 mmol, 51%) separated (Found: C, 73.35; H, 6.45; Cr, 11.30; N, 6.05. Calc. for $C_{28}H_{28}CrN_2O$: C, 73.00; H, 6.15; Cr, 11.30; N, 6.10%). IR (Nujol mull, KBr, cm^{-1}): 1585s, 1570s, 1335m, 1325w, 1305s, 1245s, 1210m, 1165s, 1140w, 1075m, 1020s, 990s, 910s, 875s, 860s, 820s, 750s, 730s, 700m, 685s, 520m, 505s and 480s. μ_{eff} = 3.58.

$[Cr(NPh_2)_2(py)_2]\cdot 0.5py$ **3a**.—A solution of $[Cr(NPh_2)_2(thf)_2]$ (1.82 g, 3.47 mmol) in thf (30 cm^3) was treated with pyridine (py) (5 cm^3). The resulting deep green solution precipitated large green crystals of compound **3a** upon cooling at −30 °C (1.22 g, 2.1 mmol, 59%) (Found: C, 74.75; H, 5.50; Cr, 8.70; N, 10.85. Calc. for $C_{36.5}H_{32.5}CrN_{4.5}$: C, 74.80; H, 5.55; Cr, 8.90; N, 10.75%). IR (Nujol mull, KBr, cm^{-1}): 1610m, 1600w, 1580s, 1440s, 1330s, 1310s, 1220s, 1180m, 1070m, 1050w, 990m, 900w, 860m, 750s, 700s, 695s, 630m, 530m and 515m. μ_{eff} = 4.76.

$[Cr(NPh_2)_2(thf)_2]$ **3b**.—Sodium hydride (0.26 g, 10.8 mmol) was suspended into a solution of diphenylamine (1.82 g, 10.8 mmol) in thf (40 cm^3) and the resulting mixture was stirred and refluxed for 30 min. After cooling to room temperature, solid $[CrCl_2(thf)_2]$ (1.41 g, 5.4 mmol) was added and the resulting red mixture was stirred for 10 h. After filtration and cooling at −30 °C, purple crystals of compound **3b** were obtained (1.83 g, 3.4 mmol, 64%) (Found: C, 71.30; H, 6.75; Cr, 9.40; N, 5.35. Calc. for $C_{32}H_{36}CrN_2O_2$: Cr, 72.15; H, 6.80; Cr, 9.75; N, 5.25%). IR (Nujol mull, KBr, cm^{-1}): 1570s, 1560m, 1330s, 1325s, 1300s, 1290s, 1220w, 1195m, 1160s, 1150w, 1060w, 1050w, 1020w, 1015s, 985m, 910w, 885w, 850s, 845m, 740s and 685s. μ_{eff} = 4.69.

$[Cr(C_{12}H_8NS)_2(thf)_2]$ **3c**.—A solution of phenothiazine ($C_{12}H_9NS$) (1.50 g, 7.6 mmol) in thf (30 cm^3) was treated with NaH (0.18 g, 7.5 mmol). After the gas evolution was complete, solid $[CrCl_2(thf)_2]$ (1.01 g, 3.8 mmol) was added to the reaction mixture. The colour turned red and stirring was continued for 10 h. The solution was filtered and its volume subsequently reduced almost to dryness. After addition of toluene (10 cm^3), deep red crystals of compound **3c** (1.17 g, 1.98 mmol, 52%) separated upon standing for 15 h at −30 °C (Found: C, 64.65; H, 5.30; Cr, 8.45; N, 4.85. Calc. for $C_{32}H_{32}CrN_2O_2S_2$: C, 64.85; H, 5.45; Cr, 8.75; N, 4.75%). IR (Nujol mull, KBr, cm^{-1}): 1575s, 1550s, 1450s, 1410m, 1320s, 1290s, 1270m, 1240m, 1210s, 1145s, 1105s, 1050m, 1020s, 1005s, 960m, 920s, 910m, 850s, 815w, 730s, 710m, 700w, 680w, 600w, 560m, 490s and 430s. μ_{eff} = 4.88.

$[Na_2Cr(NPh_2)_4(thf)_4]$ **4a**.—Solid NPh_2H (2.28 g, 13.5 mmol) was added to a suspension of NaH (0.32 g, 13.3 mmol) in thf (60 cm^3). The mixture was stirred and refluxed for 30 min to allow complete saltification. After cooling to room temperature $[CrCl_2(thf)_2]$ (0.90 g, 3.4 mmol) was added and the stirring was continued for 12 h. After solvent removal *in vacuo*, the solid residue was recrystallized from ether (40 cm^3) at −30 °C, yielding deep purple crystals of compound **4a** (1.53 g, 1.42 mmol, 42%) (Found: C, 71.85; H, 6.95; Cr, 4.80; N, 4.80; Na, 5.25. Calc. for $C_{64}H_{72}CrN_4Na_2O_4$: C, 72.55; H, 6.85; Cr, 4.90; N, 5.30; Na, 4.35%). IR (Nujol mull, KBr, cm^{-1}): 1580s, 1575s, 1320w, 1280s, 1270s, 1190s, 1160s, 1140m, 1070w, 1040s, 1020w, 985s, 900w, 890s, 880s, 870m, 830m, 810w, 740s, 695s, 690s, 610m, 525s, 500s and 420m. μ_{eff} = 4.63.

$[Li_2Cr(NEt_2)_4(thf)_2]$ **4b**.—Neat diethylamine (2.3 g, 30.8 mmol) was added dropwise to a solution of $[Li_4Cr_2Me_8(thf)_4]$ (2.04 g, 3.8 mmol) in thf (20 cm^3). The resulting brown mixture was stirred for 20 h. After solvent removal *in vacuo*, the resulting solid was redissolved in ether (15 cm^3) and filtered. Light green crystals of compound **4b** (1.63 g, 3.3 mmol, 43%) formed upon standing for 2 d at −80 °C (Found: C, 56.95; H, 11.25; Cr, 10.25; Li, 2.85; N, 11.40. Calc. for $C_{24}H_{56}CrLi_2N_4O_2$: C, 57.80; H, 11.30; Cr, 10.45; Li, 2.80; N, 11.25%). IR (Nujol mull, KBr, cm^{-1}): 1560m, 1360s, 1340s, 1280s, 1245m, 1160s, 1145m, 1095s, 1045s, 1000s, 910s, 890s, 865m, 770s, 710w and 640m. μ_{eff} = 4.91.

$[Li_2Cr(NEt_2)_4(py)_2]$ **4c**.—Neat diethylamine (1.91 g, 26.2 mmol) was added to a solution of LiMe (15.3 cm^3, 1.7 mol dm^{-3}, 26.1 mmol) in thf (50 cm^3). After the gas evolution was complete, solid $[CrCl_2(thf)_2]$ (1.73 g, 6.48 mmol) was added. The resulting dark green solution was stirred for 20 h. The volume was then reduced to 10 cm^3 and diethyl ether (20 cm^3) added. After filtration, the solution was treated with pyridine (1.5 cm^3). Large, deep green crystals of compound **4c** (2.57 g, 6.02 mmol, 78%) separated upon cooling to −30 °C (Found: C, 61.65; H, 9.75; Cr, 9.55; Li, 2.55; N, 15.85. Calc. for $C_{26}H_{50}CrLi_2N_6$: C, 60.90; H, 9.85; Cr, 10.15; Li, 2.70; N, 16.40%). IR (Nujol mull, KBr, cm^{-1}): 2830w, 1590w, 1480m,

1420s, 1330m, 1320m, 1275s, 1205s, 1165s, 1130m, 1100s, 1065m, 1050m, 1000s, 995s, 950m, 890w, 850s, 775m, 745s, 695s and 615m. μ_{eff} = 4.83.

$[Cr_2\{NMe(C_5H_4N\text{-}2)\}_4]\cdot 2thf$ **5a**.—A solution of 2-methylaminopyridine (1.68 g, 15.5 mmol) in thf (30 cm^3) was cooled to −80 °C and treated with a solution of LiMe in ether (9.7 cm^3, 1.6 mol dm^{-3}). The solution was allowed to warm to room temperature and then treated with solid $[CrCl_2(thf)_2]$ (2.07 g, 7.8 mmol). After stirring for 5 h at room temperature, the resulting orange-red suspension was evaporated *in vacuo* and the solid residue recrystallized from a mixture of hexane (75 cm^3) and thf (20 cm^3) at −30 °C, yielding brick-red crystals of compound **5a** (1.86 g, 2.75 mmol, 70.5%) (Found: C, 56.70; H, 6.80; Cr, 15.20; N, 16.35. Calc. for $C_{32}H_{44}Cr_2N_8O_2$: C, 56.80; H, 6.55; Cr, 15.35; N, 16.55%). IR (Nujol mull, KBr, cm^{-1}): 1600s, 1500w, 1410w, 1290s, 1270s, 1165m, 1150w, 1120m, 1075m, 1010m, 980w, 930w, 820s, 810s, 745s, 720s, 640m, 630s, 590w, 520s, 445s and 430s. μ_{eff} = 0.34.

$[\{Cr[N(C_5H_4N\text{-}2)_2]_2\}_2]\cdot 2dmf$ **5b**.—A solution of di-2-pyridylamine (2.63 g, 15.4 mmol) in thf (150 cm^3) was treated with NaH (0.37 g, 15.5 mmol). After the gas evolution was complete, solid $[CrCl_2(thf)_2]$ (2.02 g, 7.6 mmol) was added to the resulting suspension. The solution turned red and a red solid precipitated. After 5 h of stirring the mixture was evaporated to dryness and the solid residue was recrystallized from boiling dimethylformamide (dmf), yielding brick-red crystals of compound **5b** (2.19 g, 2.35 mmol, 62%) (Found: C, 59.25; H, 5.10; Cr, 11.30; N, 21.15. Calc. for $C_{46}H_{46}Cr_2N_{14}O_2$: C, 59.35; H, 5.00; Cr, 11.15; N, 21.05%). IR (Nujol mull, KBr, cm^{-1}): 1670m, 1610s, 1580s, 1480m, 1420m, 1310m, 1290w, 1275m, 1180s, 1145s, 1055s, 990w, 970m, 760s, 750m, 730s, 650m, 615m, 540m, 520m and 450m. ^1H NMR ($CDCl_3$): δ 8.28 (m), 8.06 (s), 7.59 (m), 6.83 (m), 2.91 (d, J = 12 Hz). μ_{eff} = 0.31.

X-Ray Crystallography.—The air-sensitive crystals used for this study were selected in a dry-box and sealed in a thin-walled glass capillary. The unit-cell parameters, obtained from least-squares refinement of 25 high-angle reflections, were checked for the presence of higher lattice symmetry.[15] The intensities of three reference reflections were measured every 3 h of X-ray exposure to monitor crystal decomposition and possible instrument instability. Space groups were derived from the observed systematic absences and checked for the presence of higher metrical symmetry.[16] The net intensities of the data were corrected for the scale variation, Lorentz and polarization effects, but not for absorption. Standard deviations as obtained by counting statistics were increased according to an analysis of the excess of variance of the three reference reflections.[17] Structures were solved by Patterson methods and subsequent partial structure expansion (SHELXS 86[18] and SHELXTL PLUS). Details of the data collection and structure refinement are in Table 1, selected bond distances and angles in Table 8. All calculations were carried out with the program packages SHELX 76,[19] XTAL,[20] EUCLID[21] and a locally modified version of PLUTO.[22]

Compound **1b**. Unit-cell parameters were obtained from setting angles of 22 reflections with 5.13 < θ < 12.89°. Positional and anisotropic thermal parameters for the non-hydrogen atoms were refined with block-diagonal least-squares procedures (XTAL).[20] The hydrogen atoms were included with their calculated positions in the final refinement riding on their carrier atoms. Weights were introduced in the final refinement cycles. Final refinement on F was carried out by full-matrix least squares with anisotropic thermal parameters for the non-hydrogen atoms and one overall thermal parameter for the hydrogen atoms. Some carbon atoms showed high thermal parameters, suggesting some disorder, which is in line with the weak scattering power of the crystal investigated. The final atomic coordinates are given in Table 2.

Compound **2**. Unit-cell parameters were determined from a least-squares treatment of the SET4 setting angles of 25 reflections with 9.0 < θ < 14.6°. Refinement on F was carried out by full-matrix least-squares techniques. All non-H atoms were refined with anisotropic thermal parameters. Hydrogen atoms were introduced in calculated positions (C–H 0.98 Å) and included in the refinement riding on their carrier atoms. A toluene solvate molecule (located on an inversion symmetry site) could not be located from Fourier difference maps unambiguously and was taken into account in the structure-factor and refinement calculations by direct Fourier transformation of the electron density in the cavity, following the BYPASS procedure.[23] Weights were introduced in the final refinement cycles. Final atomic coordinates are listed in Table 3.

Compound **3a**. Lattice parameters and their standard deviations were derived from 22 reflections in the range 6.62 < θ < 14.76° in four alternative settings.[24] The intensity data were corrected for the small decay. The solvent molecule was highly disordered. Attempts to find a satisfactory disorder model failed. Following the inclusion of the pyridine molecule, the remainder of the structure refined satisfactorily. Refinement using anisotropic thermal parameters followed by Fourier difference synthesis resulted in the location of all the non-solvent hydrogen atoms. The hydrogen atoms of the interstitial pyridine were placed at idealized positions riding on their carrier atoms, used in the structure-factor calculations, but not refined. Weights were introduced in the final refinement cycles. Refinement on F was by block-diagonal least-squares techniques with anisotropic thermal parameters for the non-hydrogen atoms and one common isotropic thermal parameter for the hydrogen atoms. Final atomic coordinates are given in Table 4.

Compound **3c**. Lattice parameters and their standard deviations were derived from 22 reflections in the range 6.02 < θ < 14.42° in four alternative settings.[24] The intensity data were corrected for the small drift. The positions and anisotropic thermal parameters for the non-hydrogen atoms were refined with block-diagonal least-squares procedures. The hydrogen atoms were included with their calculated positions in the final refinement cycle. Refinement on F by block-diagonal least-squares techniques was carried out with anisotropic thermal parameters for the non-hydrogen atoms. The crystal exhibited some secondary extinction for which the F values were corrected by refining an empirical isotropic extinction parameter.[25] Final atomic coordinates for the non-hydrogen atoms are reported in Table 5.

Compound **4c**. Unit-cell parameters were determined from a least-squares treatment of SET4 setting angles of 25 reflections with 10.7 < θ < 17.7°. Data were corrected for a linear decay (2.2%) of the intensity control reflections during the 47 h of X-ray exposure. Refinement on F was carried out with anisotropic thermal parameters. The hydrogen atom positions were isotropically refined with one common thermal parameter [U = 0.099(3) $Å^2$]. Weights were introduced in the final refinement cycles. Final atomic coordinates are listed in Table 6.

Compound **5b**. Cell constants and orientation matrix for data collection were obtained from a least-squares refinement using the setting angles of 25 carefully centred reflections in the range 24 < θ < 32°. Data were collected at room temperature using the ω-scan technique to a maximum 2θ value of 50.0°. Data were corrected for absorption. The structure was refined with full-matrix least-squares techniques. With the exception of the solvent molecule, all the non-hydrogen atoms were refined anisotropically. Final atomic coordinates are listed in Table 7.

Additional material available from the Cambridge Crystallographic Data Centre comprises H-atom coordinates, thermal parameters and remaining bond lengths and angles.

Results

The synthetic procedures used for the preparation of chromium(II) amides are briefly outlined in the following schemes.

Table 1 Crystal data and structural analysis results *

Complex	**1b**	**2**	**3a**	**3c**	**4c**	**5b**
Formula	$C_{48}H_{88}Cr_2N_4$	$C_{63}H_{64}N_4O_2Cr_2$	$C_{37.3}H_{33.3}CrN_{4.7}$	$C_{32}H_{32}CrN_2O_2S_2$	$C_{26}H_{50}CrLi_2N_6$	$C_{46}H_{46}Cr_2N_{14}O_2$
M	825.24	1031.22	599.36	592.73	512.60	931.0
Crystal system	Tetragonal	Triclinic	Monoclinic	Monoclinic	Monoclinic	Orthorhombic
Space group	$I4_1/acd$	$P\bar{1}$	$P2_1/a$	$I2/a$	$P2_1/n$	$Pbcn$
a/Å	17.285(2)	9.975(1)	18.322(2)	16.326(1)	11.072(1)	23.881(5)
b/Å		10.119(2)	9.435(2)	15.947(1)	9.326(1)	9.644(2)
c/Å	32.354(3)	13.963(2)	26.428(3)	22.428(2)	14.968(2)	19.219(3)
α/°		105.63(1)				
β/°		90.82(1)	92.800(9)	103.59(1)	94.95(1)	
γ/°		103.87(1)				
U/Å^3	9666(2)	1313.0(4)	4563(1)	5675.7(7)	1539.6(3)	4426.3(15)
Z	8	1	6	8	2	4
T/K	298	295	130	295	295	295
D_c/g cm^{-3}	1.134	1.281	1.309	1.387	1.106	1.397
μ_{calc}/cm^{-1}	4.7	4.4	4.0	5.7	3.8	5.32
R_F, R'	0.132, 0.052	0.053, 0.066	0.073, 0.056	0.081, 0.052	0.044, 0.049	0.085, 0.101

* Details in common: Mo-Kα radiation (λ 0.710 73 Å).

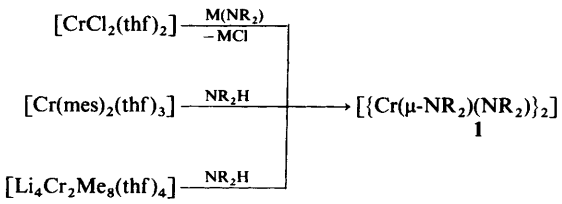

Scheme 1 R = C_6H_{11} **1b** or Pr^i **1c**; M = Na or Li; mes = 2,4,6-$Me_3C_6H_2$

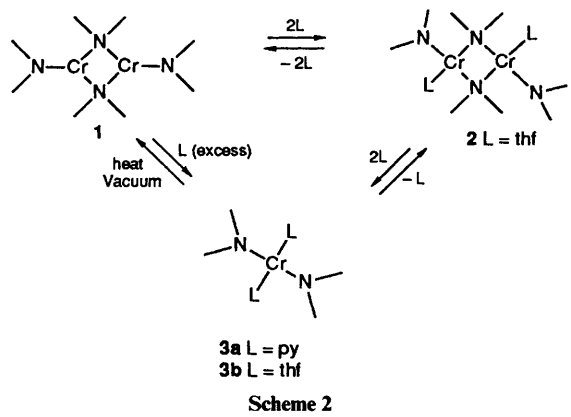

Scheme 2

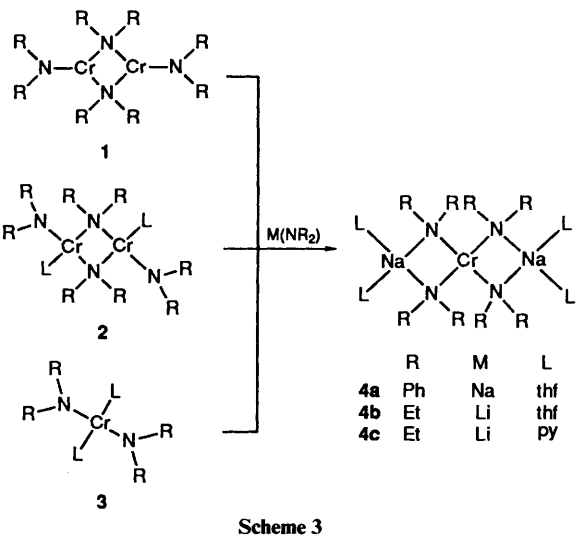

Scheme 3

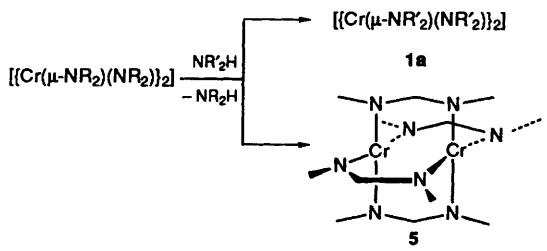

Scheme 4 R = C_6H_{11} or Pr^i; R′ = Ph **1a**, NMe(C_5H_4N-2) **5a** or $N(C_5H_4N\text{-}2)_2$ **5b**

According to Scheme 1, reaction of $[CrCl_2(thf)_2]$ with 2 equivalents of the alkali-metal amide leads to the formation of the corresponding dimeric, homoleptic $[\{Cr(\mu\text{-}NR_2)(NR_2)\}_2]$ (R = Ph **1a**, cyclohexyl **1b** or Pr^i **1c**). The same compounds were obtained upon reaction of both monomeric $[Cr(mes)_2(thf)_3]$[12] or dimeric $[Li_4Cr_2Me_8(thf)_4]$[12d,e] with the appropriate amine. The reaction proceeds directly towards the final product when R = C_6H_{11} or Pr^i. Conversely in the case of R = Ph a monomeric species which retained two molecules of solvent in the co-ordination sphere of chromium is initially formed and the dimerization reaction towards $[\{Cr(\mu\text{-}NPh)_2(NPh_2)\}_2]$ was obtained only upon solvent removal *in vacuo* at 100 °C, followed by recrystallization from hot toluene. In contrast to the two aliphatic congeners where R = C_6H_{11} or Pr^i which do not react with Lewis bases such as thf and pyridine, $[\{Cr(\mu\text{-}NPh_2)(NPh_2)\}_2]$ reacts reversibly with thf initially forming the dimeric $[\{Cr(\mu\text{-}NPh_2)(NPh_2)L\}_2]$ **2** and the monomeric $[Cr(NPh_2)_2L_2]$ **3** (L = thf), depending on the amounts of thf employed (Scheme 2). In the case of a stronger Lewis base such as pyridine there is no evidence for the formation of a complex isostructural with $[\{Cr(\mu\text{-}NPh_2)(NPh_2)(thf)\}_2]$ since the reaction proceeds directly towards the formation of the monomeric $[Cr(NPh_2)_2(py)_2]$ even in the presence of lower amounts of pyridine. An irreversible reaction was observed in the case of the phenothiazine derivative which led to the formation of monomeric $[Cr(C_{12}H_8NS)_2(thf)_2]$ in good yield.

Monomeric and dimeric chromium(II) amides **1**–**3** react with an excess of $M(NR_2)$ (M = Li or Na) to afford monomeric amidochromates $[M_2Cr(NR_2)_4L_n]$ (R = Ph, M = Na, n = 4, L = thf **4a**; R = Et, M = Li, n = 2, L = thf **4b** or pyridine **4c**) (Scheme 3). In contrast with the isostructural chromium(II) alkoxochromates,[10b,c] attempts to disrupt these complexes *via* treatment with co-ordinating solvents (pyridine, crown ethers) or to assemble dimeric species *via* desolvation of the alkali-metal cation failed.

Table 2 Fractional atomic coordinates for compound **1b**

Atom	*x*	*y*	*z*
Cr(1)	−0.058 05(8)	0.308 05(8)	−0.125 00
N(1)	−0.000 000	0.250 000(0)	0.171 4(2)
N(2)	−0.137 5(4)	0.387 5(4)	−0.125 00
C(1)	0.048 9(7)	0.298 8(6)	0.197 1(3)
C(2)	0.104 1(6)	0.257 2(6)	0.226 6(3)
C(3)	0.144 7(8)	0.317(1)	0.251 9(5)
C(4)	0.186 9(8)	0.372(1)	0.234 9(4)
C(5)	0.131 1(7)	0.415 5(6)	0.204 9(4)
C(6)	0.083 5(8)	0.359 8(7)	0.180 1(4)
C(7)	−0.121 3(7)	0.467 0(6)	0.135 8(3)
C(8)	−0.129 1(6)	0.484 6(6)	0.181 3(3)
C(9)	−0.106 2(9)	0.569 2(8)	0.190 6(4)
C(10)	−0.065(1)	0.608 8(8)	0.166 6(5)
C(11)	−0.062 2(8)	0.592 5(6)	0.123 3(4)
C(12)	−0.082 0(8)	0.511 7(7)	0.111 8(4)

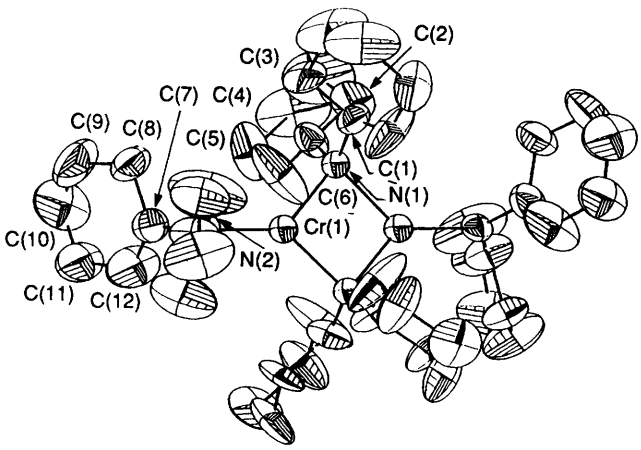

Fig. 1 An ORTEP plot of compound **1b**. Thermal ellipsoids in this and all other Figures are drawn at the 50% probability level

The complexes $[\{Cr(\mu\text{-}NR_2)(NR_2)\}_2]$ (R = C_6H_{11} or Pr^i) undergo easy transamination reactions with NPh_2H or bidentate amines such as $NMe(C_5H_4N\text{-}2)H$ or $N(C_5H_4N\text{-}2)_2H$ forming the corresponding dimeric $[\{Cr(\mu\text{-}NPh_2)(NPh_2)\}_2]$ **1a**, $[Cr_2\{NMe(C_5H_4N\text{-}2)\}_4]\cdot 2thf$ **5a** and $[\{Cr[N(C_5H_4N\text{-}2)_2]_2\}_2]\cdot 2dmf$ **5b**. The lower pK_a of these amines with respect to the aliphatic counterpart is probably the driving force for the reaction (Scheme 4). Compounds **5** can also be easily prepared *via* direct reaction of the corresponding alkali-metal amide with $[CrCl_2(thf)_2]$ although in the case of **5b** the poor solubility makes problematic the separation from the inorganic salts.

Crystal Structures.—$[\{Cr[\mu\text{-}N(C_6H_{11})_2][N(C_6H_{11})_2]\}_2]$ **1b**. The complex is isostructural with the previously reported $[\{Cr(\mu\text{-}NPr^i_2)(NPr^i_2)\}_2]$.[9c] The structure shows the molecule having a planar Cr_2N_2 core composed of two chromium and two nitrogen atoms of bridging $N(C_6H_{11})_2$ moieties (Fig. 1) [N(1)–Cr(1)–N(1a) 93.2(2), Cr–N(1)–Cr(1a) 86.8(2)°]. The geometry of the three-co-ordinated chromium atoms is distorted trigonal planar with the terminally bonded nitrogen atoms coplanar with the Cr_2N_2 core [N(1)–Cr–N(2) 133.4(1)°]. The Cr–N bond distances formed by the bridging and terminal nitrogen atoms are slightly different [Cr(1)–N(1) 2.066(5), Cr(1)–N(2) 1.942(7) Å] as a probable result of the different co-ordination geometry. The trigonal-planar arrangement of the terminal nitrogen atoms indicates, moreover, a significant N–Cr π interaction. The Cr···Cr distance [2.838(2) Å] compares well with that found in $[\{Cr(\mu\text{-}NPr^i_2)(NPr^i_2)\}_2]$.[9c]

$[\{Cr(\mu\text{-}NPh_2)(NPh_2)(thf)\}_2]$ **2**. The molecular structure is constituted by discrete dimeric units (Fig. 2). The co-ordination geometry of each chromium atom is slightly distorted square planar [N(1)–Cr(1)–O(1) 173.8(1); N(1)–Cr(1)–N(2) 97.6(1)°]. The two metals are bridged by two NPh_2 groups forming a Cr_2N_2 core [Cr(1)–N(1)–Cr(1a) 94.2(1), N(1)–Cr(1)–N(1a) 85.8(1)°] having bond distances and angles comparable to those observed in $[\{Cr(\mu\text{-}NR_2)(NR_2)\}_2]$ (R = C_6H_{11} or Pr^i). Conversely, the Cr···Cr distance is considerably longer [3.150(1) Å]. The Cr–N bond lengths formed by both the bridging and terminal μ-NPh_2 groups [Cr(1)–N(1) 2.145(3), Cr(1)–N(2) 2.031(3) Å] are slightly longer than those found in $[\{Cr(\mu\text{-}NR_2)(NR_2)\}_2]$ (R = C_6H_{11} or Pr^i) probably as a result of the decreased character of nitrogen N→Cr π bonding, determined by the two phenyl substituents. The fourth co-ordination site is occupied by one molecule of thf.

Table 3 Fractional atomic coordinates for compound **2**

Atom	*x*	*y*	*z*
Cr(1)	0.061 70(5)	0.595 90(5)	0.107 61(4)
O(1)	0.129 4(3)	0.819 0(2)	0.168 0(2)
N(1)	0.001 0(3)	0.373 5(3)	0.031 6(2)
N(2)	0.111 2(3)	0.579 5(3)	0.244 8(2)
C(1)	0.112 5(3)	0.308 5(3)	0.006 7(2)
C(2)	0.118 3(4)	0.177 8(3)	0.021 0(3)
C(3)	0.225 2(4)	0.117 1(4)	−0.012 9(3)
C(4)	0.328 5(4)	0.182 9(5)	−0.061 1(3)
C(5)	0.325 3(4)	0.311 4(5)	−0.075 0(3)
C(6)	0.219 8(4)	0.373 1(4)	−0.041 3(3)
C(7)	−0.103 8(3)	0.306 5(3)	0.086 1(2)
C(8)	−0.243 3(3)	0.276 5(3)	0.052 4(3)
C(9)	−0.347 0(4)	0.224 0(4)	0.107 8(3)
C(10)	−0.314 5(5)	0.197 4(5)	0.194 6(3)
C(11)	−0.176 0(4)	0.223 4(4)	0.227 6(3)
C(12)	−0.072 3(4)	0.278 0(4)	0.174 5(3)
C(13)	0.029 9(4)	0.638 2(4)	0.317 0(3)
C(14)	−0.112 7(4)	0.608 1(4)	0.296 0(3)
C(15)	−0.195 1(4)	0.678 6(5)	0.360 9(3)
C(16)	−0.135 5(5)	0.777 4(5)	0.449 7(3)
C(17)	0.003 7(5)	0.804 4(5)	0.472 7(3)
C(18)	0.086 8(4)	0.736 6(4)	0.408 3(3)
C(19)	0.220 1(3)	0.532 7(3)	0.274 5(3)
C(20)	0.330 3(4)	0.519 9(4)	0.213 8(3)
C(21)	0.437 0(4)	0.466 9(4)	0.238 4(3)
C(22)	0.440 9(5)	0.427 4(5)	0.325 3(4)
C(23)	0.335 1(5)	0.438 1(5)	0.385 3(4)
C(24)	0.225 4(4)	0.489 3(4)	0.361 7(3)
C(25)	0.044 9(5)	0.914 3(4)	0.213 2(4)
C(26)	0.139 9(6)	1.047 0(5)	0.267 2(4)
C(27)	0.275 5(6)	1.027 6(5)	0.271 3(5)
C(28)	0.270 6(4)	0.881 9(4)	0.214 7(3)

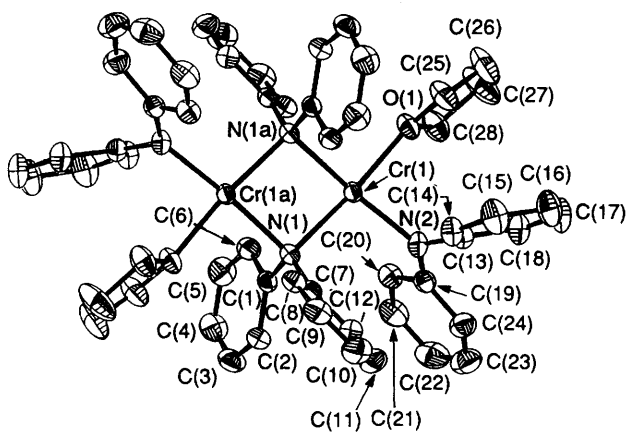

Fig. 2 An ORTEP plot of compound **2**

$[Cr(NPh_2)_2(py)_2]\cdot 0.5py$ **3a**. The unit cell contains two crystallographically independent but chemically equivalent molecules. One of the two molecules has the metal atom lying

Table 4 Fractional atomic coordinates for compound **3a**

Atom	*x*	*y*	*z*
Cr(1)	0.5	0.5	0.0
N(1)	0.5179(2)	0.6957(5)	0.0405(2)
N(2)	0.5639(2)	0.3991(5)	0.553(2)
C(1)	0.5776(3)	0.7201(7)	0.696(2)
C(2)	0.5934(3)	0.8476(8)	0.0934(2)
C(3)	0.5416(3)	0.9553(7)	0.0894(2)
C(4)	0.4785(3)	0.9323(7)	0.599(3)
C(5)	0.4683(3)	0.8035(7)	0.0358(2)
C(6)	0.6378(3)	0.3709(7)	0.0496(2)
C(7)	0.6770(3)	0.2628(7)	0.0768(2)
C(8)	0.7483(3)	0.2347(7)	0.0683(3)
C(9)	0.7857(3)	0.3098(7)	0.0315(3)
C(10)	0.7472(3)	0.4136(8)	0.0048(2)
C(11)	0.6756(3)	0.4444(7)	0.0133(2)
C(12)	0.5312(3)	0.3684(6)	0.1008(2)
C(13)	0.5658(3)	0.3839(7)	0.1485(2)
C(14)	0.5305(4)	0.3601(7)	0.1919(2)
C(15)	0.4566(3)	0.3232(7)	0.1902(2)
C(16)	0.4219(3)	0.3053(7)	0.1434(3)
C(17)	0.4752(3)	0.3275(7)	0.1000(2)

Table 5 Fractional atomic coordinates for compound **3c**

Atom	*x*	*y*	*z*
Cr(1)	0.000 00(0)	0.500 00(0)	0.000 00(0)
S(1)	−0.008 6(2)	0.555 8(2)	−0.222 8(1)
O(1)	−0.095 0(3)	0.423 4(4)	−0.048 5(2)
N(1)	0.018 8(3)	0.544 6(4)	−0.080 1(2)
C(1)	0.075 8(4)	0.504 7(5)	−0.108 4(3)
C(2)	0.074 0(4)	0.505 3(6)	−0.170 5(3)
C(3)	0.132 5(4)	0.462 6(5)	−0.194 5(4)
C(4)	0.194 6(5)	0.414 6(5)	−0.157 6(4)
C(5)	0.198 5(4)	0.411 4(5)	−0.094 9(4)
C(6)	0.141 8(4)	0.457 7(5)	−0.071 4(4)
C(7)	−0.030 1(4)	0.611 1(5)	−0.111 0(3)
C(8)	−0.045 4(4)	0.626 9(5)	−0.174 4(3)
C(9)	−0.095 4(4)	0.693 2(5)	−0.201 0(4)
C(10)	−0.132 5(5)	0.742 7(6)	−0.164 8(4)
C(11)	−0.119 4(4)	0.728 4(5)	−0.103 0(4)
C(12)	−0.068 6(4)	0.665 4(5)	−0.076 4(4)
C(13)	−0.135 0(5)	0.356 5(6)	−0.022 5(4)
C(14)	−0.194 4(5)	0.312 8(6)	−0.070 4(4)
C(15)	−0.206 4(5)	0.368 3(6)	−0.125 1(4)
C(16)	−0.130 3(5)	0.424 8(6)	−0.114 4(3)

Table 6 Fractional atomic coordinates for compound **4b**

Atom	*x*	*y*	*z*
Cr	0.5	0.5	0
N(1)	0.2317(3)	0.0888(3)	0.0012(2)
N(2)	0.3588(2)	0.4149(3)	−0.0916(2)
N(3)	0.4078(2)	0.3884(3)	0.0992(2)
Li	0.3241(6)	0.2801(6)	0.0016(4)
C(1)	0.1777(4)	0.0282(4)	−0.0724(3)
C(2)	0.1180(4)	−0.1000(5)	−0.0718(3)
C(3)	0.1115(4)	−0.1700(5)	0.0057(3)
C(4)	0.1660(4)	−0.1125(5)	0.0807(3)
C(5)	0.2238(4)	0.0160(5)	0.0772(3)
C(6)	0.3873(3)	0.3476(4)	−0.1749(2)
C(7)	0.4714(4)	0.2227(5)	−0.1578(3)
C(8)	0.2579(3)	0.5142(4)	−0.1092(2)
C(9)	0.1333(4)	0.4474(5)	−0.1187(3)
C(10)	0.4765(3)	0.2958(4)	0.1635(2)
C(11)	0.5471(4)	0.1829(4)	0.1169(3)
C(12)	0.3252(3)	0.4795(4)	0.1445(3)
C(13)	0.2095(4)	0.4092(6)	0.1681(3)

on an inversion centre and is represented in Fig. 3. The monomeric unit shows the same *trans* square-planar co-ordination geometry [N(1)–Cr(1)–N(2) 88.6(2), N(1)–Cr(1)–N(2a) 91.4(2)°] previously observed in the bulky aryl $[Cr(mes)_2L_2]$ (L = PR_3 or thf),[12b] alkoxide $[Cr(OC_6H_2Me\text{-}4\text{-}Bu^t_2\text{-}2,6)_2(thf)_2]$,[10b] amide $[Cr\{N(SiMe_3)_2\}_2(thf)_2]$[9a] and pyrrolyl $[Cr(NC_4H_2Me_2\text{-}2,5)_2(py)_2]$ derivatives.[26] The Cr–N bond lengths [Cr(1)–N(2) 2.060(5) Å] are normal and comparable to those of the other chromium(II) amides reported in this work and those observed in $[Cr\{N(SiMe_3)_2\}(thf)_2]$.[9a]

Table 7 Fractional atomic coordinates for compound **5b**

Atom	*x*	*y*	*z*
Cr(1)	4 655(1)	5 888(2)	2 236(1)
N(1)	5 740(4)	7 318(10)	2 138(5)
N(2)	4 894(4)	7 507(9)	1 628(5)
N(3)	4 035(4)	7 345(11)	1 124(6)
N(4)	4 939(4)	4 492(9)	1 507(5)
N(5)	5 674(4)	4 259(10)	2 221(5)
N(6)	6 422(5)	4 611(12)	2 909(6)
C(1)	6 286(5)	7 651(12)	2 206(7)
C(2)	6 544(5)	8 608(14)	1 771(7)
C(3)	6 236(5)	9 215(14)	1 246(7)
C(4)	5 695(6)	8 878(13)	1 163(6)
C(5)	5 426(6)	7 939(12)	1 633(6)
C(6)	4 461(5)	8 178(13)	1 292(6)
C(7)	4 420(6)	9 602(14)	1 171(7)
C(8)	3 952(7)	10 119(16)	876(9)
C(9)	3 528(7)	9 296(19)	675(8)
C(10)	3 574(6)	7 919(18)	812(7)
C(11)	4 660(6)	4 223(13)	908(6)
C(12)	4 853(6)	3 288(14)	413(6)
C(13)	5 337(6)	2 589(13)	535(6)
C(14)	5 622(5)	2 886(13)	1 131(7)
C(15)	5 426(5)	3 822(11)	1 632(6)
C(16)	6 156(5)	3 724(13)	2 512(7)
C(17)	6 328(6)	2 328(15)	2 474(7)
C(18)	6 798(8)	1 887(22)	2 781(8)
C(19)	7 098(7)	2 802(25)	3 143(9)
C(20)	6 884(8)	4 173(23)	3 212(8)
O	2 621(7)	1 928(17)	−53(8)
N(7)	2 967(6)	3 788(14)	−581(7)
C(21)	3 033(10)	2 860(28)	−57(13)
C(22)	2 471(13)	3 697(29)	−992(12)
C(23)	3 464(11)	4 615(27)	−574(12)

Table 8 Selected bond distances (Å) and angles (°)

Complex 1b			
Cr(1)–N(1)	2.066(5)	N(1)–Cr(1)–N(2)	133.4(1)
Cr(1)–N(2)	1.942(7)	Cr(1)–N(1)–Cr(1a)	86.8(2)
Cr(1) · · · Cr(1a)	2.838(2)	N(1)–Cr(1)–N(1a)	93.2(2)
Complex 2			
Cr(1)–N(1)	2.145(3)	N(1)–Cr(1)–O(1)	173.8(1)
Cr(1)–N(2)	2.031(3)	N(1)–Cr(1)–N(1a)	85.8(1)
Cr(1) · · · Cr(1a)	3.150(1)	N(1)–Cr(1)–N(2)	97.6(1)
Complex 3a			
Cr(1)–N(2)	2.060(5)	N(1)–Cr(1)–N(2)	88.6(2)
Cr(1)–N(1)	2.152(5)	N(1)–Cr(1)–N(2a)	91.4(2)
Complex 3c			
Cr(1)–N(1)	2.022(5)	N(1)–Cr(1)–O(1)	89.5(2)
		O(1)–Cr(1)–N(1b)	90.5(2)
Complex 4c			
Cr–N(2)	2.141(2)	Li–N(2)–Cr	87.6(2)
Cr–N(3)	2.142(2)	N(1)–Li–N(2)	133.6(3)
N(2)–Cr–N(3)	84.17(9)	N(1)–Li–N(3)	131.1(3)
N(2')–Cr–N(3)	95.83(9)	N(2)–Li–N(3)	95.3(3)
Complex 5b			
Cr(1)–N(2)	2.032(9)	N(1a)–Cr(1)–N(2)	87.1(4)
Cr(1)–N(4)	2.059(9)	N(2)–Cr(1)–N(4)	91.1(4)
Cr(1)–Cr(1a)	1.937(3)		

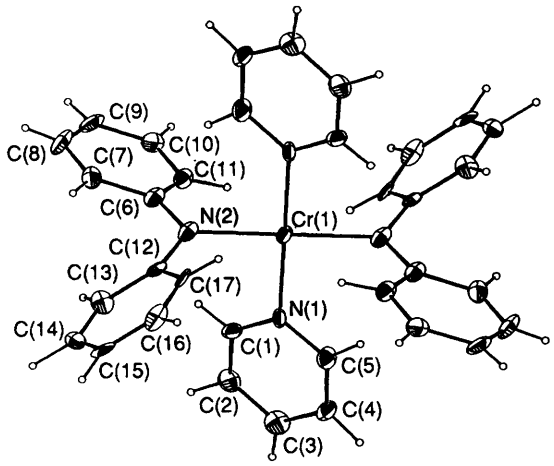

Fig. 3 An ORTEP plot of compound **3a**

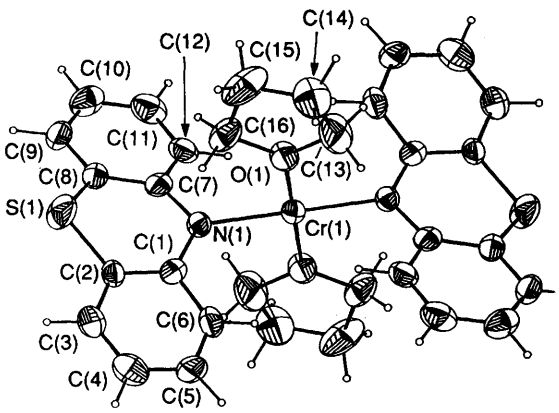

Fig. 4 An ORTEP plot of compound **3c**

The two residual pyridine ligands are coplanar to each other, whereas the Cr–N bond length [Cr(1)–N(1) 2.152(5) Å] compares well with those observed in other chromium(II) complexes.[26] The second crystallographically independent molecule does not have an inversion centre. However the bond distances and angles are comparable.

$[Cr(C_{12}H_8NS)_2(thf)_2]$ **3c**. The unit cell contains two crystallographically independent but chemically equivalent molecules. In both cases the molecule is formed by discrete monomeric units with a central chromium atom in an almost perfect square-planar *trans* configuration geometry [N(1)–Cr(1)–O(1) 89.5(2), O(1)–Cr(1)–N(1b) 90.5(2)°] (Fig. 4). The two nearly planar molecules of phenothiazine are positioned perpendicular to the CrO_2N_2 plane. The Cr–N distances [Cr(1)–N(1) 2.022(5) Å] are shorter than in $[Cr(NPh_2)_2(py)_2]$·0.5py. The two thf rings positioned *trans* to each other are nearly coplanar with the CrN_2O_2 molecular core. All the bond distances and angles are as expected.

$[Li_2Cr(NEt_2)_4(py)_2]$ **4c**. The molecule is composed of a square-planar $(R_2N)_4Cr$ dianion binding two lithium cations through the nitrogen atoms of the amido groups, in an overall planar arrangement of the Li_2CrN_4 core (Fig. 5). The co-ordination geometry around the central chromium atom is square planar [N(2)–Cr–N(3) 84.17(9), N(2′)–Cr–N(3) 95.83(9)°]. The Cr–N distances [Cr–N(2) 2.141(2), Cr–N(3) 2.142(2) Å] are quite normal and comparable to those found in all the other chromium(II) amides reported in this work. Each lithium atom possesses a distorted trigonal co-ordination geometry [N(1)–Li–N(2) 133.6(3), N(1)–Li–N(3) 131.1(3), N(2)–Li–N(3) 95.3(3)°], the third co-ordination site being occupied by a molecule of pyridine. The angle subtended at the nitrogen atom by the Cr and Li atoms [Li–N(2)–Cr 87.6(2)°] is similar to that observed in $[\{Cr[\mu\text{-}N(C_6H_{11})_2][N(C_6H_{11})_2]\}_2]$.

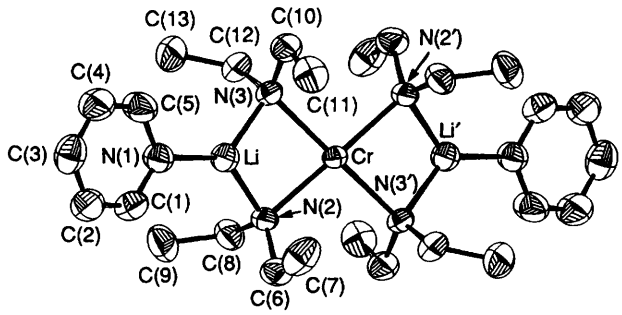

Fig. 5 An ORTEP plot of compound **4c**

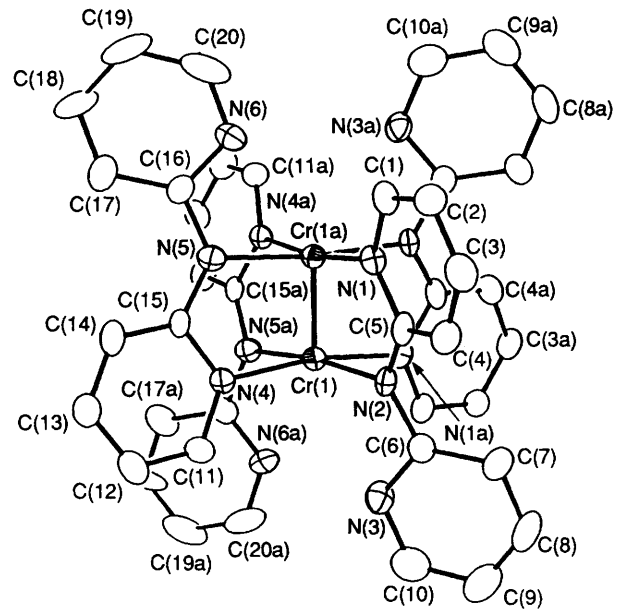

Fig. 6 An ORTEP plot of compound **5b**

Two ethyl groups of two NEt_2 moieties are bent towards the fourth and fifth co-ordination sites of an ideal trigonal bipyramid centred on lithium, with fairly short Cr···H distances involving one of the two CH_2 groups [Cr···H(82) 2.831(3), Cr···H(121) 2.854(4) Å].

$[\{Cr[N(C_5H_4N\text{-}2)_2]_2\}_2]$·2dmf **5b**. The structure of the complex shows the molecule to have the typical dimeric arrangement (lantern type) of the well known quadruply bonded complexes of dichromium (Fig. 6). The molecule is formed by a Cr_2 moiety bridged by four amido ligands placed *trans* with respect to each other, and with the two planes defined by each pair of *trans*-positioned ligands which are perpendicular. Each ligand adopts the classical three-centre chelating geometry, where each of the two donor atoms of one ligand molecule binds one of the two metal centres of the Cr_2 unit, forming a five-membered ring. In common with the so-called supershort quadruply bonded systems, the co-ordination geometry around the two chromium atoms is square planar [N(1a)–Cr(1)–N(2) 87.1(4), N(2)–Cr(1)–N(4) 91.1(4)°] with the chromium atoms slightly intruded into the co-ordination polyhedron [distance of Cr(1) from the N(1a),N(2),N(4),N(5a) plane is 0.143(1) Å]. The Cr–N bonding distances [Cr(1)–N(2) 2.032(9), Cr(1)–N(4) 2.059(9) Å] are quite normal and compare well with those found in $[Cr_2(NC_5H_3NH\text{-}2\text{-}Me\text{-}6)_4]$[27] and $[Cr_2(C_7H_5N_2)_4\ (dmf)_2]$ ($C_7H_6N_2$ = 7-azaindole).[26] The Cr(1)···Cr(1a) 1.937(3) Å is considerably short and falls in the range of the supershort Cr···Cr contacts.

Discussion

Although both monomeric and quadruply bonded dimeric chromium(II) complexes have been used for the preparation of

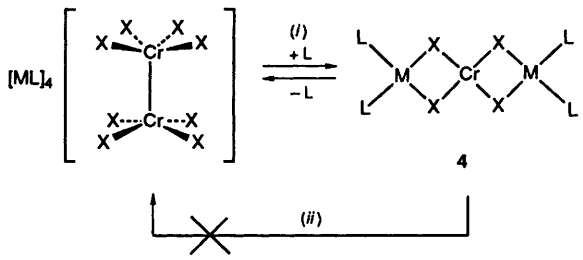

Scheme 6 (*i*) X = Me, OPh or OPr^i, M = Na or Li, L = thf, Et_2O or py; (*ii*) X = NR_2, M = Li

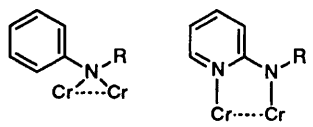

Scheme 7 R = aryl

chromium(II) amides (Scheme 1), with the aim of investigating the tendency of chromium to form or to preserve metal–metal bonds, the result of the reaction was not affected by the choice of starting material. In both cases the dimeric homoleptic $[\{Cr(NR_2)_2\}_2]$ was the only reaction product. This result may be ascribed to high stability of the Cr_2N_2 core, which might also be related to the presence of a Cr···Cr bond. The fairly short Cr···Cr distances found in $[\{Cr(\mu\text{-}NR_2)(NR_2)\}_2]$ [2.838 (R = C_6H_{11}) and 2.866 Å (R = Pr^i) respectively] and the low-spin electronic configurations (μ_{eff} = 2.62 and 2.30 respectively)[9c] suggest, in fact, a significant degree of M···M bonding (single or double). However, simple treatment with a weak Lewis base (thf) gave a remarkable increase in the intermetallic distance (up to 3.150 Å in $[\{Cr(\mu\text{-}NPh_2)(NPh_2)(thf)\}_2]$) while preserving the $Cr_2(NR_2)_2$ core, and significantly modified the magnetic moment (μ_{eff} = 3.58). Since the Cr···Cr distances and the magnetic properties of the metal respond so strongly to simple solvent co-ordination, the Cr···Cr interaction is probably very weak in these complexes and certainly not able to hold together the dimetallic framework in the absence of bridging donor atoms. In other words, the role of the Cr···Cr bond in the stabilization of the dimetallic unit should be only minor. In agreement with these observations, treatment with a slight excess of co-ordinating solvent (thf or pyridine) gave facile cleavage of the $Cr_2(NR_2)_2$ core, forming monomeric, square-planar $[Cr(NR_2)_2L_2]$ species with the expected high-spin d^4 electronic configuration (μ_{eff} = 4.68).

The Lewis acidity of alkali-metal cations is a factor which has been shown to be responsible for holding together di- and poly-metallic frameworks of chromium(II) species.[4a,10c] However, attempts to prepare dimeric anionic amidochromates $Li_4Cr_2(NR_2)_8$, isostructural with alkyl[12d,e] (with supershort Cr···Cr quadruple bonds) and alkoxide derivatives (without Cr···Cr bonds)[10c] gave only monomeric $[M_2Cr(NR_2)_4(thf)_2]$ (M = Li or Na) derivatives (Scheme 6), despite these species being isostructural with the monomeric alkoxide and alkyl building blocks of the corresponding dimers. The failure of $[M_2Cr(NR_2)_4(thf)_2]$ to dimerize is probably due to either the poor ability of the amide nitrogen donor atom to give the μ_3-bonding mode necessary for assembling $Li_4Cr_2(NR_2)_8$, or steric congestion as suggested by the short CH_2CH_3···Li contacts and the trigonal co-ordination geometry of the lithium cation observed in $[Li_2Cr(NEt_2)_4(py)_2]$. However, when the three-centre chelating geometry is introduced in the amide ligand, for example just by placing a donor atom (nitrogen) in the *ortho* position of the aromatic rings of Ph_2N (Scheme 7), and therefore introducing only a minor alteration in the overall steric bulk of the bridging amide ligand, a very short Cr···Cr contact [1.937(3) Å], the characteristic 'lantern type' framework and the very low residual paramagnetism of the well known quadruply bonded systems were observed as expected for the resulting dimeric chromium(II) amide derivative $[\{Cr[N(C_5H_4N\text{-}2)_2]_2\}_2]\cdot 2dmf$.

Acknowledgements

This work was supported by the Natural Sciences and Engineering Research Council of Canada (operating grant) and the Petroleum Research Funds administered by the American Chemical Society (PRF 22770-AC3). The Nederlandse Organisatie voor Wetenschappelijk Onderzoek (NWO) is gratefully acknowledged for providing a visiting scholarship (to J. J. H. E.) and for supporting part of the crystallographic work (A. L. S. and W. J. J. S.).

References

1 C. C. Cummings, S. M. Baxter and P. T. Wolczanski, *J. Am. Chem. Soc.*, 1988, **116**, 8731.
2 R. I. LaDuca and P. T. Wolczanski, *Inorg. Chem.*, 1992, **31**, 1311.
3 M. D. Fryzuk, T. S. Haddad and S. J. Rettig, *J. Am. Chem. Soc.*, 1990, **112**, 8185.
4 (*a*) R. Duchateau, S. Gambarotta, N. Beydhoun and C. Bensimon, *J. Am. Chem. Soc.*, 1991, **113**, 8986; (*b*) N. Beydhoun, R. Duchateau and S. Gambarotta, *J. Chem. Soc., Chem. Commun.*, 1992, 244.
5 D. C. Bradley, M. B. Hursthouse, K. M. A. Malik and R. Moseler, *Transition Met. Chem. (Weinheim, Ger.)*, 1978, **3**, 253 and refs. therein; M. F. Lappert, P. P. Power, A. R. Sanger and R. C. Srivastava, *Metal and Metalloid Amides*, Ellis Horwood, Chichester, 1980 and refs. therein.
6 G. Wilkinson, *Comprehensive Coordination Chemistry*, Pergamon, Oxford, 1987.
7 W. E. Buhro, M. H. Chisholm, K. Folting, J. C. Huffman, J. D. Martin and W. E. Streib, *J. Am. Chem. Soc.*, 1992, **114**, 557 and refs. therein; W. E. Buhro, M. H. Chisholm, J. D. Martin, J. C. Huffman, K. Folting and W. E. Streib, *J. Am. Chem. Soc.*, 1989, **111**, 8149 and refs. therein; T. P. Blatchford, M. H. Chisholm and J. C. Huffman, *Inorg. Chem.*, 1987, **26**, 1920; M. H. Chisholm, J. C. Huffman and C. A. Smith, *J. Am. Chem. Soc.*, 1986, **108**, 222.
8 K. J. Ahmed, M. H. Chisholm, K. Folting and J. C. Huffman, *J. Am. Chem. Soc.*, 1986, **108**, 989; M. H. Chisholm, B. W. Eichhorn and J. C. Huffman, *Organometallics*, 1987, **6**, 2264.
9 (*a*) D. C. Bradley, *Chem. Br.*, 1975, **11**, 393; (*b*) R. A. Bartlett, H. Chen and P. P. Power, *Angew. Chem.*, 1989, **101**, 325; (*c*) J. J. H. Edema, S. Gambarotta and A. L. Spek, *Inorg. Chem.*, 1989, **28**, 811.
10 (*a*) J. J. H. Edema, S. Gambarotta, P. van der Sluis, W. J. J. Smeets and A. L. Spek, *Inorg. Chem.*, 1989, **28**, 3782; (*b*) J. J. H. Edema, S. Gambarotta, F. van Bolhuis, W. J. J. Smeets and A. L. Spek, *Inorg. Chem.*, 1989, **28**, 1407; (*c*) J. J. H. Edema, S. Gambarotta, F. van Bolhuis and A. L. Spek, *J. Am. Chem. Soc.*, 1989, **111**, 2142; (*d*) J. J. H. Edema, S. Gambarotta, W. J. J. Smeets and A. L. Spek, *Inorg. Chem.*, 1991, **30**, 1380; (*e*) J. J. H. Edema and S. Gambarotta, *Comments Inorg. Chem.*, 1991, **11**, 195; (*f*) J. J. H. Edema, S. Gambarotta, F. Bolhuis, W. J. J. Smeets and A. L. Spek, *Inorg. Chem.*, 1989, **28**, 1407; (*g*) S. Hao, S. Gambarotta and C. Bensimon, *J. Am. Chem. Soc.*, 1992, **113**, 3556; (*h*) S. Hao, J. J. H. Edema and S. Gambarotta, *Inorg. Chem.*, 1992, **31**, 2676.
11 F. H. Kohler and W. Prossdorf, *Z. Naturforsch., Teil B*, 1977, **32**, 1026.
12 (*a*) M. Tsutsui and H. Zeiss, *J. Am. Chem. Soc.*, 1960, **82**, 6255; (*b*) A. R. Hermes, R. J. Morris and G. S. Girolami, *Organometallics*, 1988, **7**, 2372; (*c*) J. J. H. Edema, S. Gambarotta, F. van Bolhuis, W. J. J. Smeets, A. L. Spek and M. Y. Chiang, *J. Organomet. Chem.*, 1990, **389**, 47; (*d*) J. Krausse, G. Mark and G. Schoedl, *J. Organomet. Chem.*, 1970, **21**, 159; (*e*) J. Krausse and G. Schoedl, *J. Organomet. Chem.*, 1971, **27**, 59.
13 M. B. Mabbs and D. J. Machin, *Magnetism and Transition Metal Complexes*, Chapman Hall, London, 1973.
14 G. Foese, C. J. Gorter and L. J. Smits, *Constantes Selectionnées Diamagnetisme, Paramagnetisme, Relaxation Paramagnetique*, Masson, Paris, 1957.
15 A. L. Spek, *J. Appl. Crystallogr.*, 1988, **21**, 578.
16 L. E. McCandlish, G. H. Stout and L. C. Andrews, *Acta Crystallogr., Sect. A*, 1975, **31**, 245.
17 Y. Le Page, *J. Appl. Crystallogr.*, 1987, **20**, 264.
18 G. M. Sheldrick, SHELXS 86, Program for crystal structure solution, University of Göttingen, 1986.

19 G. M. Sheldrick, SHELX 76, Crystal structure analysis package, University of Cambridge, 1976.
20 *XTAL 2.6 User's Manual*, eds S. R. Hall and J. M. Stewart, Universities of Western Australia and Maryland.
21 A. L. Spek, in *Computational Crystallography*, ed. D. Sayre, Clarendon Press, Oxford, 1982, p. 528.
22 A. Meetsma, Extended version of the program PLUTO, University of Groningen, unpublished work.
23 P. van der Sluis and A. L. Spek, *Acta Crystallogr., Sect. A*, 1990, **46**, 194.
24 J. L. de Boer and A. J. M. Duisenberg, *Acta Crystallogr., Sect. A*, 1984, **40**, C410.
25 W. H. Zachariansen, *Acta Crystallogr.*, 1967, **23**, 558.
26 J. J. H. Edema, S. Gambarotta, A. Meetsma, F. van Boluis, A. L. Spek and W. J. J. Smeets, *Inorg. Chem.*, 1990, **29**, 2147.
27 F. A. Cotton, R. H. Niswander and J. C. Sekutowski, *Inorg. Chem.*, 1978, **17**, 3541.

Received 23*rd June* 1992; *Paper* 2/03300C